Electronic Supplementary Information

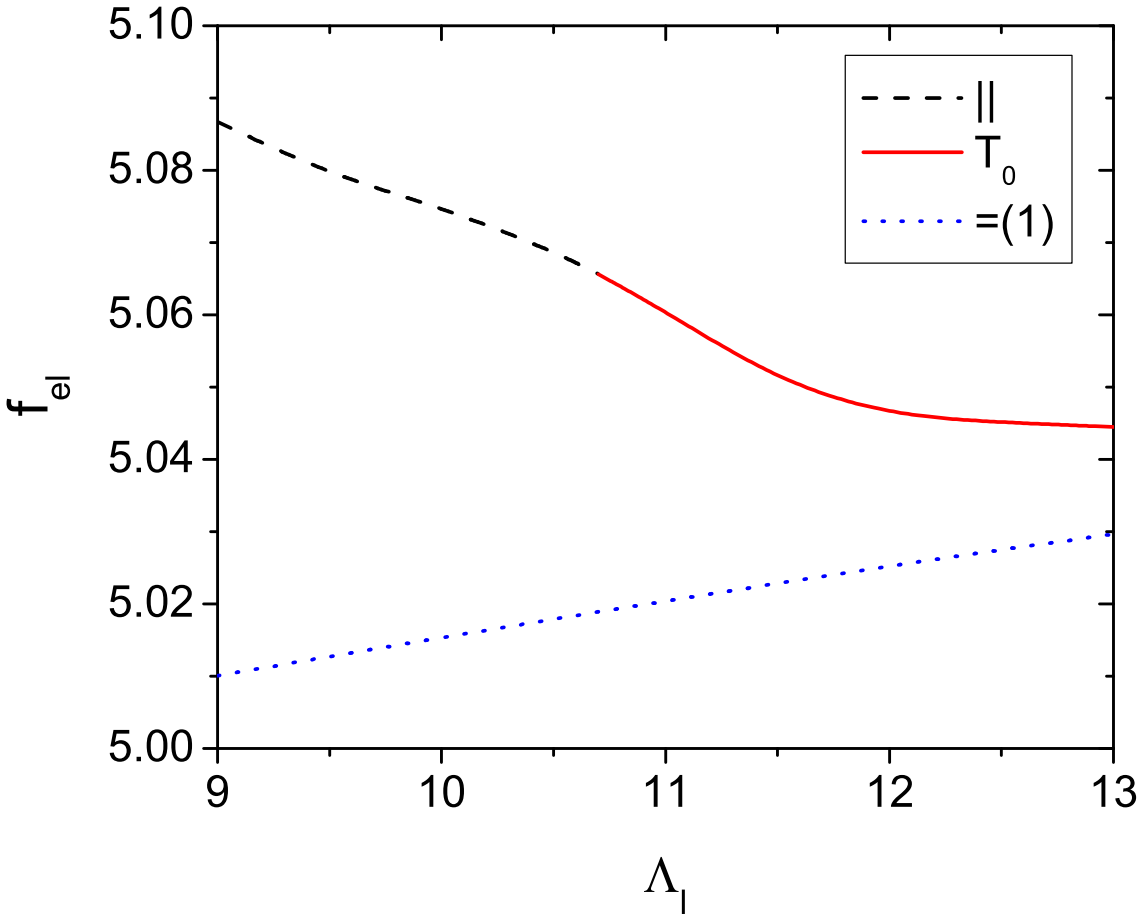

Figure 3: (c)

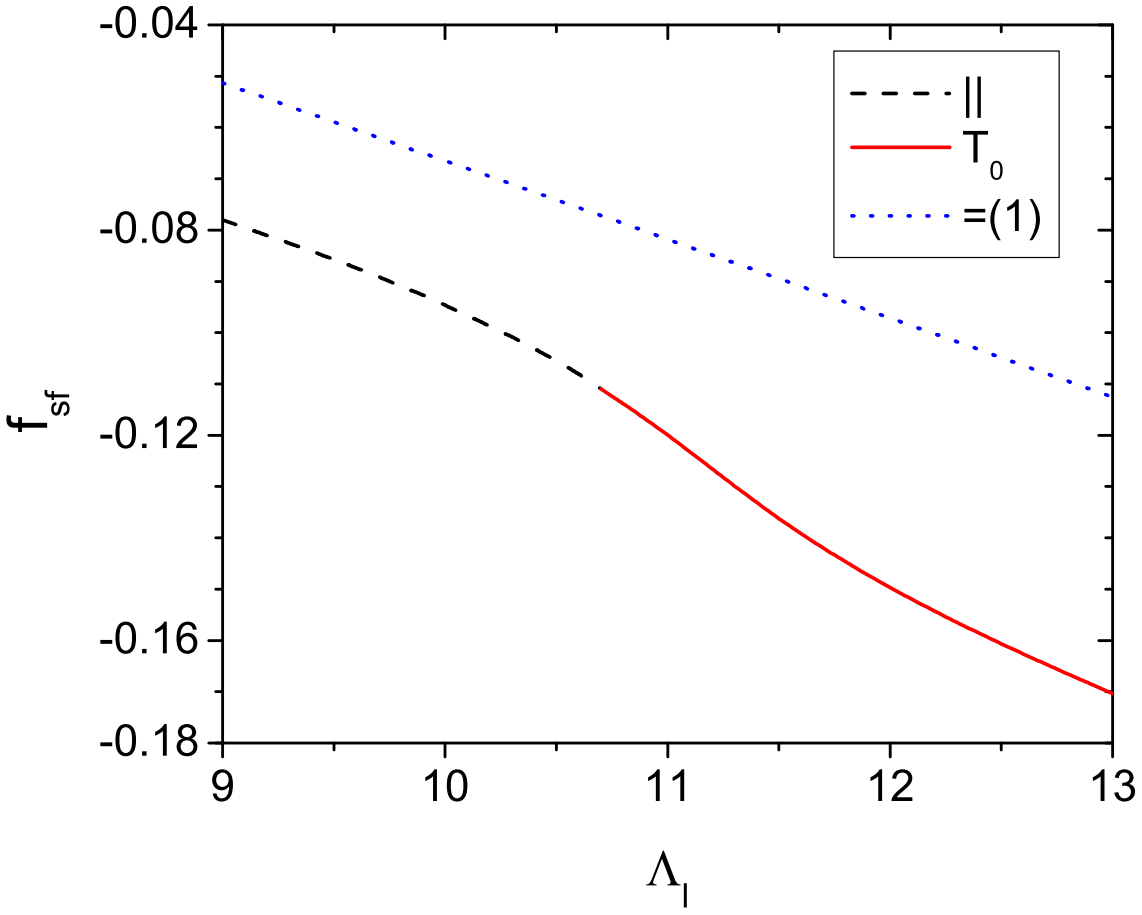

Figure 3: (d)

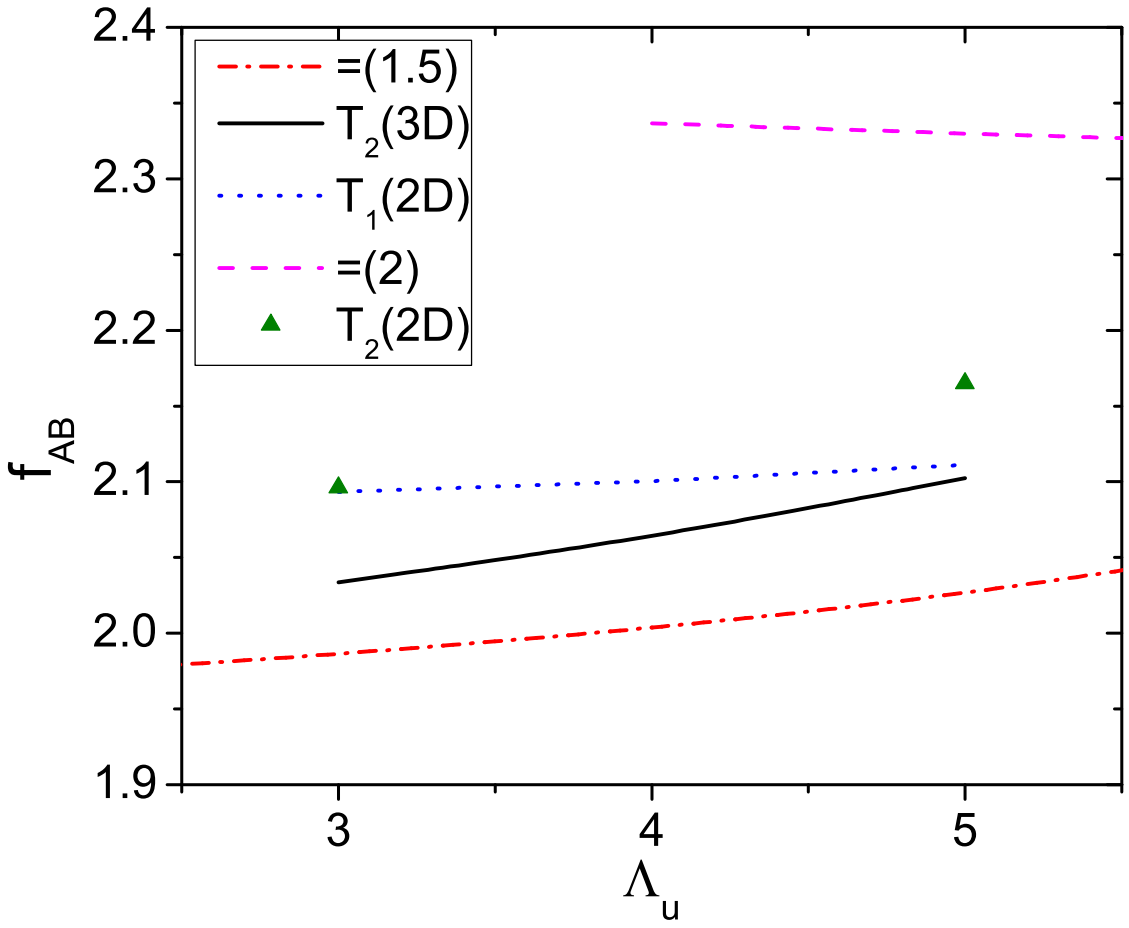

Figure 14: (b)

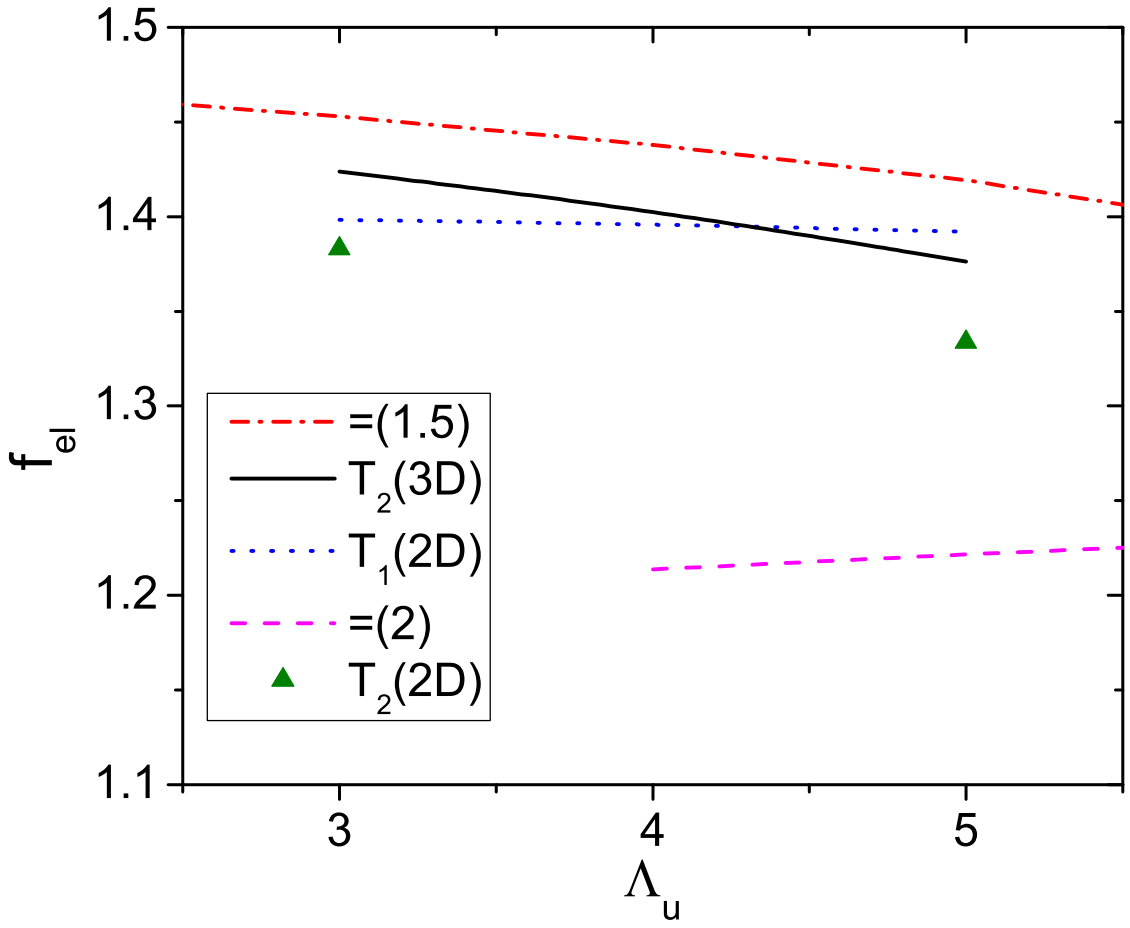

Figure 14: (c)

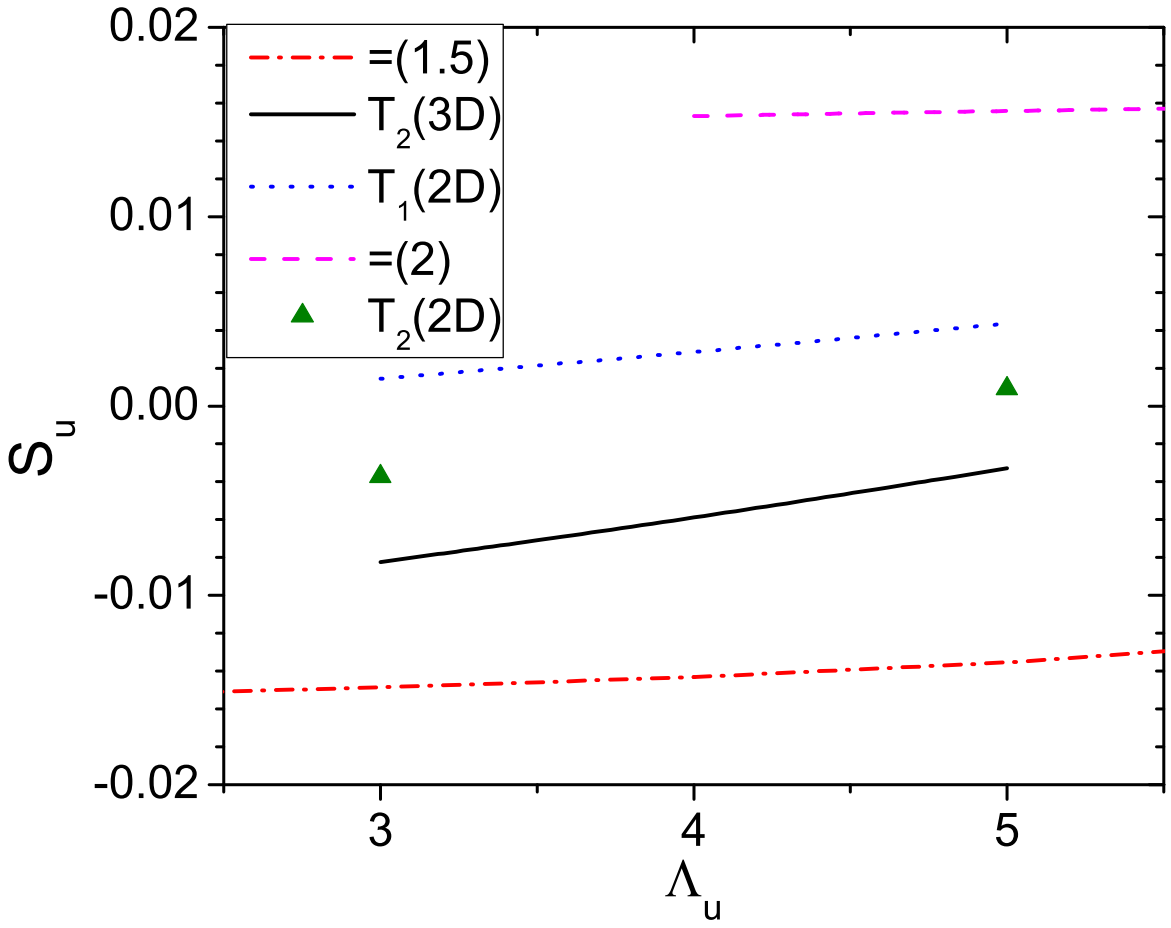

Figure 14: (d)

Accuracy of Free-Energy Calculations

Obviously, the accuracy of our calculated free energy per chain f_c determines the reliability of our constructed phase diagrams. This accuracy depends on several factors, including the cell length and its discretization (number of subintervals) m in each dimension, the chain contour discretization n, and the convergence criterion ϵ for iterating SCF equations. The choice of m, n and ϵ are dictated by the boundary conditions in the confined dimension and the sharpness of A-B interfaces in each dimension (i.e., χN and the morphology). When the Dirichlet boundary conditions are used, the accuracy is mainly determined by the spatial discretization in the confined dimension, and the detailed numerical analysis in our previous work[31] justifies our statement that an accuracy of $< 10^{-3}$ in f_c is reached in our calculations.

When the Neumann boundary conditions are used, the accuracy is mainly determined by the sharpness of A-B interfaces. We therefore perform 1D calculations of =(1) between two neutral surfaces separated at $D = L_0$ (our bulk calculations at $\chi N = 20$ give $L_0 \approx 4.045 R_g$, in good agreement with Ref. [27]). The results shown in Fig. 15 clearly justify our statement that an accuracy of $< 10^{-3}$ in f_c is reached in our calculations. Note that the A-B interfaces in =(1.5) under the same conditions are smoother, resulting in higher accuracy in f_c (data not shown).

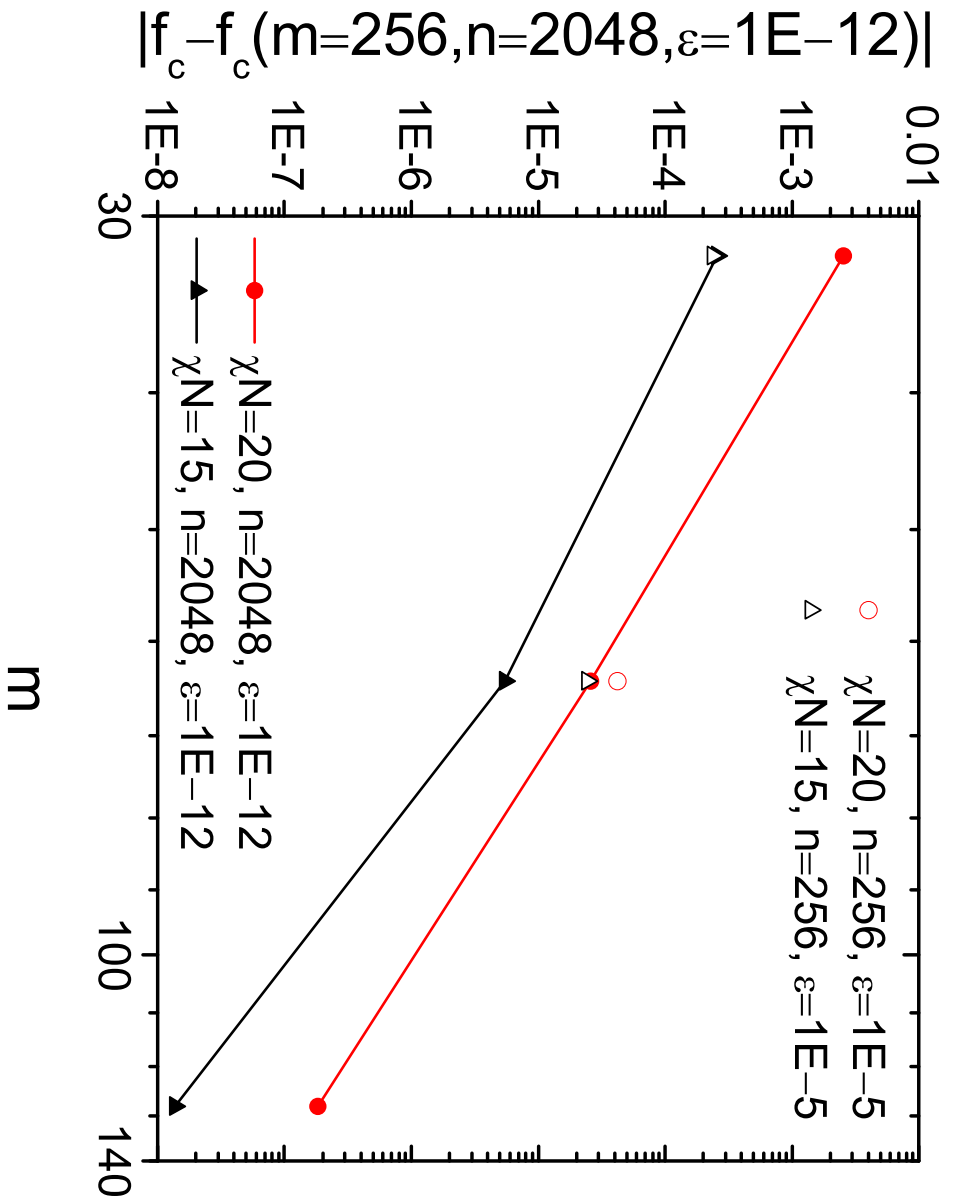

Figure 15: Accuracy of the obtained free energy per chain f_c in 1D calculations of =(1) between two neutral surfaces separated at $D = L_0$ without the hard-surface effect.

Stability of $\mathbf{T_1}$ at $\boldsymbol{\chi N = 20}$

Using the same discretization and convergence criterion as given in Sec. 2, we have performed some calculations of L_0-thick films between dissimilar surfaces without the hard-surface effect, where we set $\chi N = 20$ and $\Lambda_l = 10$. Fig. 16 compares the obtained free energies of =(1), =(1.5), T_1(2D) and T_1(3D); the results are qualitatively the same as those shown in Fig. 10, including all the free-energy components (data not shown). Our results in Sec. 3.2 (including those on the lateral periods of T_1; data not shown) therefore remain valid at $\chi N = 20$. Comparing to Fig. 7 at $\chi N = 15$, we find that both the stable regions of T_1(2D) and T_1(3D) over parallel lamellae shrink and are shifted to larger $|\Lambda_u|$-values with increasing χN, and that T_1(2D) is no longer stable against T_1(3D) at $\chi N = 20$ due to its too large f_{AB} (data not shown).

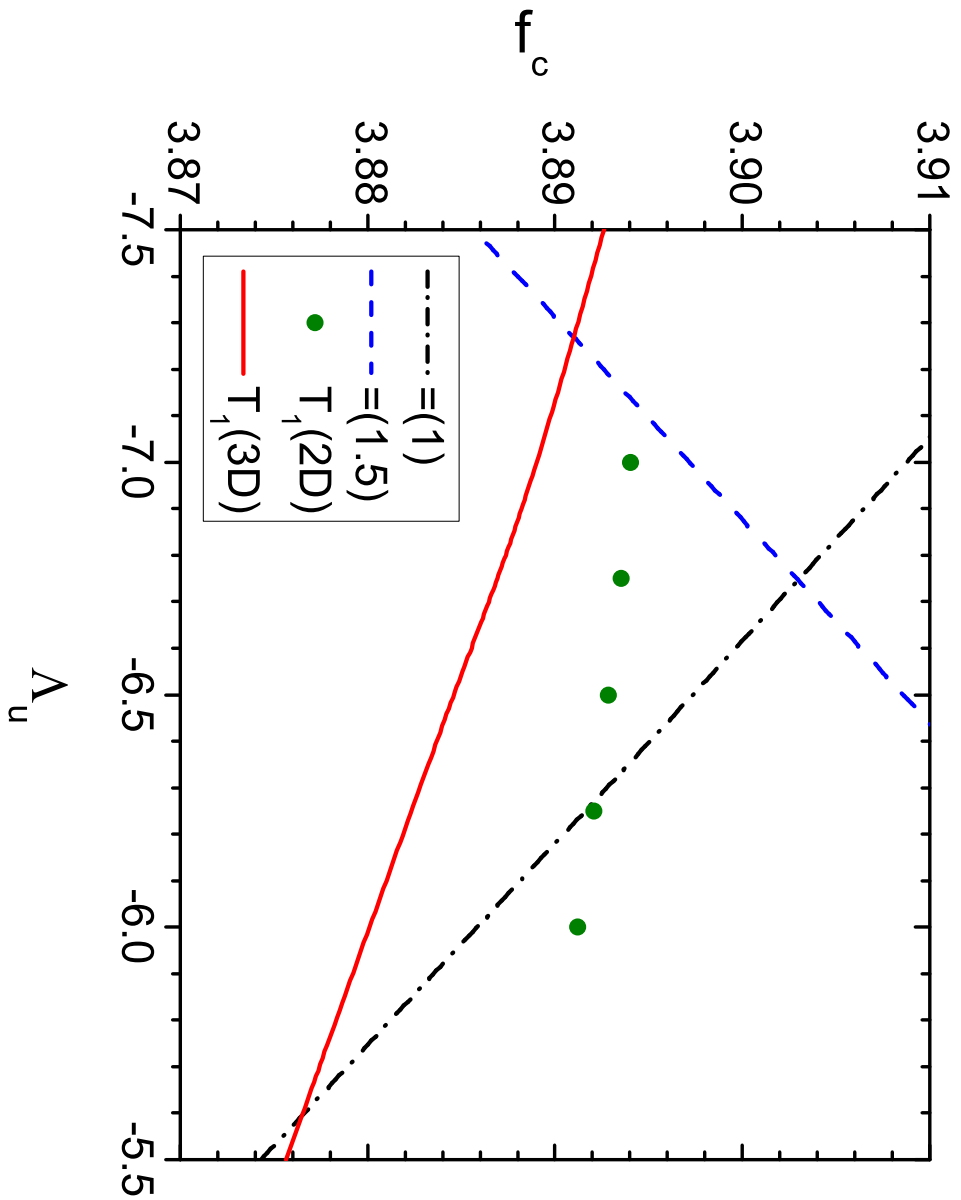

Figure 16: Free energy per chain f_c of various morphologies at $\chi N = 20$, $D = L_0 \approx 4.045R_g$ and $\Lambda_l = 10$ obtained from 3D calculations without the hard-surface effect.